Time-skew error correction in two-channel time-interleaved ADCs based on a two-rate approach and polynomial impulse responses

Anu Kalidas Muralidharan Pillai and Håkan Johansson

Linköping University Post Print

Tweet

N.B.: When citing this work, cite the original article.

©2012 IEEE. Personal use of this material is permitted. However, permission to reprint/republish this material for advertising or promotional purposes or for creating new collective works for resale or redistribution to servers or lists, or to reuse any copyrighted component of this work in other works must be obtained from the IEEE.

Anu Kalidas Muralidharan Pillai and Håkan Johansson, Time-skew error correction in two-channel time-interleaved ADCs based on a two-rate approach and polynomial impulse responses, 2012, Proc. IEEE 55th Int. Midwest Symp. Circuits Syst. (MWSCAS), 1136-1139.
http://dx.doi.org/10.1109/MWSCAS.2012.6292225

Postprint available at: Linköping University Electronic Press
http://urn.kb.se/resolve?urn=urn:nbn:se:liu:diva-84307

Time-Skew Error Correction in Two-Channel Time-Interleaved ADCs Based on a Two-Rate Approach and Polynomial Impulse Responses

Anu Kalidas Muralidharan Pillai and Håkan Johansson
Division of Electronics Systems, Department of Electrical Engineering, Linköping University, SE-581 83, Sweden
Email: {kalidas, hakanj}@isy.liu.se

***Abstract*— Even though time-interleaved analog-to-digital converters (ADCs) help to achieve higher bandwidth with simpler individual ADCs, gain, offset, and time-skew mismatch between the channels degrade the achievable resolution. Of particular interest is the time-skew error between channels which results in nonuniform samples and thereby introducing distortion tones at the output of the time-interleaved ADC. Time-varying digital reconstructors can be used to correct the time-skew errors between the channels in a time-interleaved ADC. However, the complexity of such reconstructors increases as their bandwidth approaches the Nyquist band. In addition to this, the reconstructor needs to be redesigned online every time the time-skew error varies. Design methods that result in minimum reconstructor order require expensive online redesign while those methods that simplify online redesign result in higher reconstructor complexity. This paper proposes a technique that can be used to simplify the online redesign and achieve a low complexity reconstructor at the same time.**

I. Introduction

A time-interleaved analog-to-digital converter (TI-ADC) consists of multiple channels in parallel, where each channel ADC operates at a lower rate compared to the sampling rate of the TI-ADC [1]. The final output of the TI-ADC is formed by interleaving the outputs from all the channels. Such time-interleaving helps to reduce the requirements on the individual channel ADC since they operate at a lower rate. The sampling clocks to the individual ADCs are applied in such a way that at any sampling instant, only one ADC samples the input. This is achieved by introducing a uniform time-skew between the clocks applied to the different ADCs. However, due to non-idealities, the time-skew between ADC clocks will not be uniform as shown in Fig. 1. Such static time-skew errors results in a periodic nonuniformly sampled sequence at the output of the TI-ADC and degrades the effective resolution. Hence, a reconstructor is used to convert the nonuniformly sampled sequence to a uniformly sampled sequence.

At high sampling frequencies, the time-skew errors will be frequency-dependent [2], [3] and need special reconstruction methods [4]. However, in this paper, we assume that the operating frequency is not very high and hence the time-skew error can be considered to be static. The design of reconstructors that make use of time-varying discrete-time FIR filters was addressed in detail in [5]. The design approach in [5] gives reconstructors with minimum order but if the time-skew error varies, all the coefficients in the reconstructor have to be redesigned. This requires all the coefficient multipliers in the reconstructor to be implemented using variable coefficient multipliers whose complexity is higher compared to fixed coefficient multipliers. Also, the implementation complexity of the online filter design block as well as the power consumption due to variable updates increases as the number of coefficients to be redesigned increases. The reconstructor design method proposed in [6] utilizes polynomial impulse response FIR filters to eliminate the need for online redesign. Reconstructors designed with [6] use very few variable multipliers but need significantly larger number of fixed multipliers. A two-rate based approach was suggested in [7] which resulted in a reconstructor that needed fewer fixed multipliers compared to [6] and fewer variable coefficient multipliers that require online redesign compared to [5]. In this paper, we extend the two-rate approach in [7] to obtain a structure that doesn't require online redesign.

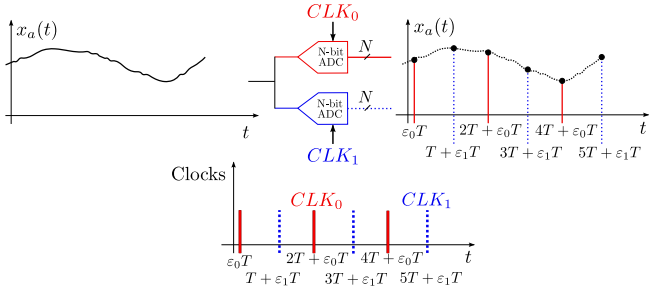

Fig. 1. Nonuniform sampling in two-channel TI-ADC.

After this introduction, in Section II, we review the details of periodic nonuniform sampling and reconstruction using time-varying FIR filters. Section III explains the basic two-rate approach and shows two structures that can be used to implement the designed reconstructor. Section IV outlines the steps to design a two-rate based polynomial impulse response reconstructor. In Section V, with the help of a design example, the complexity of the reconstructor designed using the proposed method is compared with that obtained using [5], [6], and [7]. Section VI concludes the paper.

II. Periodic Nonuniform Sampling and Reconstruction

A continuous-time signal, $x_a(t)$, when uniformly sampled results in a discrete-time sequence given by

$$x(n) = x_a(nT) \tag{1}$$

where nT is the uniform sampling instant and T is the sampling period. In a two-channel TI-ADC, the final output is formed by interleaving the outputs from both the channels. Hence, for uniformly sampled signals at the output of a TI-ADC, there should be a time-skew of T between the sample clocks of the two channels. However, timing mismatches between the two channels will result in an error in the time-skew causing a nonuniformly sampled signal at the TI-ADC output. If ε_n denotes the percentage deviation of the actual time-skew from the desired value of nT for the nth sample and $v(n)$ represents the nonuniformly sampled sequence at the output of the TI-ADC for a continuous-time input signal $x_a(t)$, then

$$v(n) = x_a(nT + \varepsilon_n T). \tag{2}$$

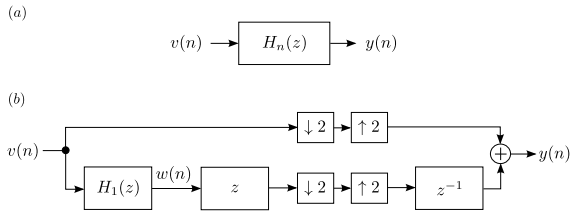

Fig. 2. (a) Time-varying reconstruction filter. (b) Equivalent two-channel filter-bank representation when $H_0(z) = 1$.

Since the output of the two-channel TI-ADC is formed by interleaving the outputs from each channel and if we assume that the time-skew error remains constant for a block of samples, then the time-skew error can be considered as two-periodic. Hence, if ε_0 and ε_1 are the time-skew errors of the first and second channel of the TI-ADC, then $\varepsilon_{2n} = \varepsilon_0$ and $\varepsilon_{2n+1} = \varepsilon_1$, for all values of n.

A perfect reconstructor converts the nonuniformly sampled signal $v(n)$ to the uniformly sampled sequence $x(n)$. However, in practice, it is not feasible to implement such a perfect reconstruction system. The reconstructor considered in this paper is a time-varying discrete-time FIR system whose output, $y(n)$, approximates the uniformly sampled signal, $x(n)$. If $h_n(k)$ is the impulse response of the reconstructor (assumed to be noncausal with even order, to simplify derivations), then

$$y(n) = \sum_{k=-N}^{N} v(n-k)h_n(k). \tag{3}$$

In the two-channel TI-ADC, the impulse response of the reconstructor will be two-periodic such that $h_n(k) = h_{n+2}(k)$. Since the reconstructor is used to correct the relative time-skew error between the channels, we assume that $\varepsilon_0 = 0$ and ε_1 represents the difference in time-skew error between the second channel and the first channel. This implies that for even n, $v(n)$ should be passed to the output as such since $h_0(k) = \delta(k)$. As shown in the two-channel maximally decimated filter-bank representation of the reconstructor in Fig. 2(b), the first channel should be passed as such while the time-skew error in the second channel should be corrected using the reconstructor $H_1(z)$ whose impulse response is $h_1(k)$. Hence, the reconstructor design procedure aims at identifying $h_1(k)$ such that the error $e(n) = y(n) - x(n)$ is minimized. It was shown in [5] that if $x_a(t)$ bandlimited to ω_0 and if $X(e^{j\omega T})$ is the Fourier transform of the uniformly sampled sequence $x(n)$, then

$$y(n) = \frac{1}{2\pi} \int_{-\omega_0 T}^{\omega_0 T} A_n(j\omega T) X(e^{j\omega T}) e^{j\omega T n} d(\omega T) \tag{4}$$

where

$$A_n(j\omega T) = \sum_{k=-N}^{N} h_n(k) e^{-j\omega T(k-\varepsilon_{n-k})}. \tag{5}$$

Also it can be shown that for perfect reconstruction [5],

$$A_n(j\omega T) = 1, \;\; \omega T \in [-\omega_0 T, \omega_0 T]. \tag{6}$$

For a two-channel TI-ADC, since $\varepsilon_0 = 0$ and $h_0(k) = \delta(k)$, $A_0(j\omega T) = 1$ and the coefficients of $h_1(k)$ should be chosen such that the error between $A_1(j\omega T)$ and 1 is minimized for a given bandwidth, $\omega_0 T$, and time-skew error, ε_1.

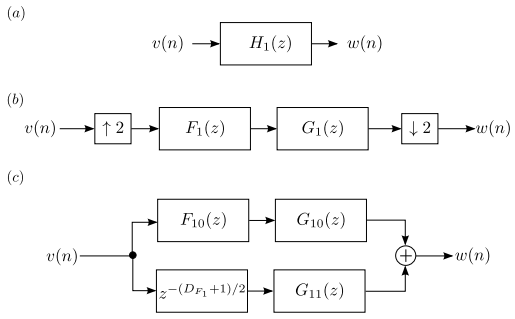

Fig. 3. (a) Transfer function of the reconstructor for the second channel of a two-channel TI-ADC. (b) Basic two-rate approach where $F_1(z)$ is a half-band filter. (c) Equivalent single-rate realization of (b) using polyphase components of $F_1(z)$ and $G_1(z)$.

III. Two-rate Based Approach

Figure 3(b) shows how the basic two-rate approach can be used to split $H_1(z)$ in Fig. 3(a) into a linear-phase half-band filter, $F_1(z)$, and a low complexity reconstructor, $G_1(z)$. If $F_{10}(z)$ and $F_{11}(z)$ are the polyphase components of $F_1(z)$ and if $G_{10}(z)$ and $G_{11}(z)$ are the polyphase components of $G_1(z)$, using multirate theory [8], the two-rate structure in Fig. 3(b) can be replaced with the single-rate structure shown in Fig. 3(c). Since $F_1(z)$ is a linear-phase half-band filter, the polyphase component $F_{11}(z)$ is equal to a delay $z^{-(D_{F_1}-1)/2}$, where D_{F_1} is the delay of $F_1(z)$. Comparing Fig. 3(a) and Fig. 3(c),

$$\begin{aligned} H_1(z) &= F_{10}(z)G_{10}(z) + z^{-1}F_{11}(z)G_{11}(z) \\ &= F_{10}(z)G_{10}(z) + z^{-(D_{F_1}+1)/2}G_{11}(z). \end{aligned} \tag{7}$$

In order to eliminate the need for online redesign, $F_{10}(z)$ is designed such that it can be used for all values of time-skew error between $\pm\varepsilon_1$. The filter $G_1(z)$ is implemented using polynomial impulse response FIR filters so that the coefficients of the impulse response need not be redesigned whenever time-skew error varies between $\pm\varepsilon_1$. Expressing the impulse response of $G_1(z)$ as an Rth-order polynomial in ε_1, we get

$$g_1(k) = \sum_{r=0}^{R} \alpha_1^{(r)}(k)\varepsilon_1^r. \tag{8}$$

Assuming $\varepsilon_{1,max} = -\varepsilon_{1,min}$, we can impose symmetry constraint for the coefficients, $\alpha_1^{(r)}$, such that

$$\alpha_1^{(r)}(k) = \alpha_1^{(r)}(-k), \text{ for even } r \tag{9}$$

and

$$\alpha_1^{(r)}(k) = -\alpha_1^{(r)}(-k), \text{ for odd } r. \tag{10}$$

Since odd r results in an anti-symmetric filter,

$$\alpha_1^{(r)}(0) = 0, \text{ for odd } r. \tag{11}$$

Also, since the first stage is a pure delay,

$$\alpha_1^{(0)}(k) = \begin{cases} 1, & k = 0 \\ 0, & k \neq 0 \end{cases}. \tag{12}$$

The transfer function of $G_1(z)$ is given by

$$G_1(z) = \sum_{r=0}^{R} Q_1^{(r)}(z)\varepsilon_1^r \tag{13}$$

where

$$Q_1^{(r)}(z) = \sum_{k=-L}^{L} \alpha_1^{(r)}(k) z^{-k}. \tag{14}$$

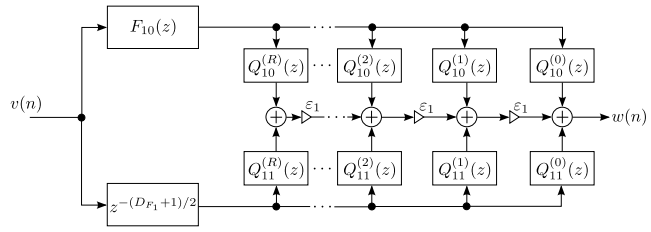

Fig. 4. Reconstructor for the second channel of two-channel TI-ADC using polynomial impulse response FIR structure for $G_{10}(z)$ and $G_{11}(z)$.

It is assumed that the order of the filter $G_1(z)$ and hence $Q_1^{(r)}(z)$ is $2L$. The symmetry constraints help in reducing the number of coefficients to be designed and implemented. However, it also requires that the order of the $G_1(z)$ should be even. The polyphase components of $G_1(z)$ can be expressed as

$$G_{10}(z) = \sum_{r=0}^{R} Q_{10}^{(r)}(z)\varepsilon_1^r \tag{15}$$

and

$$G_{11}(z) = \sum_{r=0}^{R} Q_{11}^{(r)}(z)\varepsilon_1^r \tag{16}$$

where $Q_{10}^{(r)}(z)$ and $Q_{11}^{(r)}(z)$ are the polyphase components of $Q_1^{(r)}(z)$. Since the order of $Q_1^{(r)}(z)$ is even, its polyphase components are also symmetric or anti-symmetric. Using (15) and (16), the subfilters $G_{10}(z)$ and $G_{11}(z)$ in Fig. 3(c) can be replaced with $Q_{10}^{(r)}(z)$ and $Q_{11}^{(r)}(z)$ as shown in Fig. 4.

The structure in Fig. 4 implies that, for an R-stage implementation of $G_{10}(z)$ and $G_{11}(z)$, we need only R variable multipliers. When the time-skew error varies, the variable multipliers can be directly updated with the new value of the time-skew error while the coefficients of $Q_{10}^{(r)}(z)$ and $Q_{11}^{(r)}(z)$ remain unchanged. This eliminates the need for online filter design. If the order of $F_{10}(z)$ is $2M-1$ and the filter $G_1(z)$ is implemented with an R-stage polynomial impulse response structure with each stage having an order of $2L$, we need R variable multipliers and $M+R\times L+\lfloor R/2 \rfloor$ fixed multipliers. If we compare the structure in Fig. 4 with the reconstructor in [6], it can be seen that all the multipliers in Fig. 4 operate at the input rate while the multipliers in [6] operate at half the input rate. The structure shown in Fig. 5(a) utilizes polyphase components of $G_{10}(z)$ and $G_{11}(z)$ which in turn are implemented using the polyphase components of $Q_{10}^{(r)}(z)$ and $Q_{11}^{(r)}(z)$ in (15) and (16), respectively. Here the multipliers in $F_{10}(z)$ operates at the full input rate while the multipliers in $G_{100}(z)$, $G_{101}(z)$, $G_{110}(z)$, and $G_{111}(z)$ operate at half the input rate. Hence, for the structure in Fig. 5(a), we need a total of $2M+R\times L+\lfloor R/2 \rfloor$ fixed and R variable multipliers at half the input rate. Figure 5(b) shows another possible structure where the subfilters $G_{10}(z)$ and $G_{11}(z)$ operate at the input rate while each polyphase component of $F_{10}(z)$ operate at half the input rate. Hence, the structure in Figure 5(b) needs $M+2(R\times L+\lfloor R/2 \rfloor)$ fixed multipliers and $2R$ variable multipliers at half the input rate [1].

IV. Reconstructor Design

The subfilters, $F_{10}(z)$, $G_{10}(z)$, and $G_{11}(z)$, can be designed together using a single optimization procedure. However, the cascade

[1] $D_{F_1}+1$ is assumed to be a multiple of 4. Although the number of delays will be slightly different when $D_{F_1}+1$ is not a multiple of 4, the overall structure will be similar with the same number of multipliers.

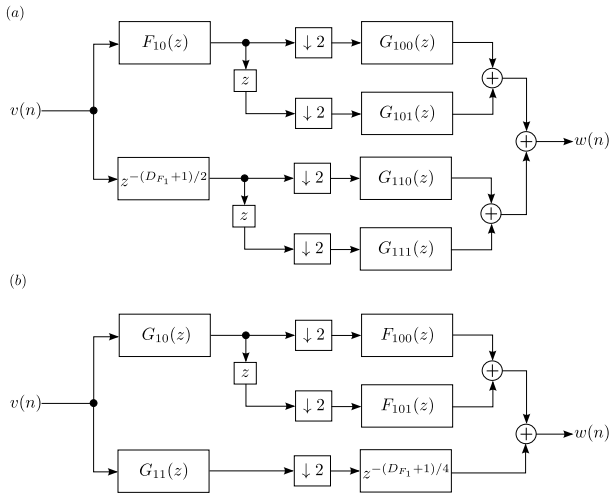

Fig. 5. Lower rate implementation of the structure in Fig. 4. (a) Multipliers in $F_{10}(z)$ operate at input rate while for each polyphase components of $G_{10}(z)$ and $G_{11}(z)$, the multipliers operate at half the input rate. (b) Multipliers in $G_{10}(z)$ and $G_{11}(z)$ operate at input rate while for each polyphase component of $F_{10}(z)$, the multipliers operate at half the input rate.

of the subfilters result in a nonlinear optimization problem and to avoid a poor local optimum, it is beneficial to split the design of the subfilters. Hence, the reconstructor design consists of two steps: design of $F_{10}(z)$ for the extreme time-skew errors $-\varepsilon_{1,max}$ and $\varepsilon_{1,max}$, and design of polynomial impulse response FIR filters for $G_{10}(z)$ and $G_{11}(z)$ with a fixed $F_{10}(z)$ over all time-skew errors between $-\varepsilon_{1,max}$ and $\varepsilon_{1,max}$.

A. Design of $F_{10}(z)$

In order to identify the coefficients of $F_{10}(z)$, we make use of the fact that as the magnitude of the time-skew error reduces from the extremes, the sampled sequence becomes less nonuniform and a lower order reconstructor can be used to obtain the same reconstruction error [5]. If $F_{10}(z)$ is designed for the extreme magnitude of time-skew error, $\varepsilon_{1,max}$, then as time-skew error varies, only the coefficients of $G_{10}(z)$ and $G_{11}(z)$ need modification. In order to design $F_{10}(z)$ using a least-squares approach, the reconstructor design problem can be stated as:

Given the orders of the subfilters $F_{10}(z)$, $G_{10}(z)$, and $G_{11}(z)$, as well as $\varepsilon_{1,max}$, determine the coefficients of these subfilters and a parameter δ, to minimize δ subject to

$$\frac{1}{2\pi}\int_{-\omega_0 T}^{\omega_0 T} |A_1(j\omega T)-1|^2 d(\omega T) \le \delta. \tag{17}$$

The filter coefficients thus designed satisfy the maximum tolerable reconstruction error (δ_e) if after optimization, $\delta \le \delta_e$. Equation (17) is a nonlinear optimization problem since $H_1(z)$ is formed by cascading two subfilters. Hence, using a good starting point for the subfilter coefficients will help in avoiding a poor local optimum.

The following steps are used to identify the coefficients of $F_1(z)$:

1) Determine the order, $\widetilde{N}_{F_1}$, of a standard half-band linear-phase FIR filter $F_1(z)$ with passband edge $\Omega_c = \omega_0 T/2$, stopband edge $\Omega_s = \pi - \Omega_c$, and with the maximum ripple in the passband and stopband being $\sqrt{\delta_e}$.
2) Determine the order, $\widetilde{N}_{G_1}$, of a filter $G_1(z)$ such that this filter approximates a regular reconstructor with error $\sqrt{\delta_e}$ and bandwidth Ω_c.

3) For each combination of N_{F_1} and N_{G_1} around the values of $\widetilde{N}_{F_1}$ and $\widetilde{N}_{G_1}$:
   (a) Design a regular half-band filter, $F_1(z)$, whose first polyphase component will give the coefficients of $F_{10}(z)$.
   (b) Set the midtap of $G_1(z)$ to one and all other taps to zero and, using polyphase decomposition, obtain the coefficients for $G_{10}(z)$ and $G_{11}(z)$.
   (c) By using the coefficients for $F_{10}(z)$, $G_{10}(z)$, and $G_{11}(z)$ determined in Steps 3(a) and 3(b) as the initial values, determine the subfilter coefficients by solving the optimization problem in (17). If δ obtained from the optimization routine is smaller than δ_e, save the results.
4) From all the results in Step 3(c) that satisfied the requirement, choose the one with lowest complexity as the final solution. In case multiple results have the same total number of multipliers, select the one with least values for N_{G_1}.

B. Design of $Q_{10}^{(r)}(z)$ and $Q_{11}^{(r)}(z)$

By defining the error power function P_1 [6] as

$$P_1 = \frac{1}{2\varepsilon_{1,max}} \frac{1}{2\pi} \int_{-\varepsilon_{1,max}}^{\varepsilon_{1,max}} \int_{-\omega_0 T}^{\omega_0 T} |A_1(j\omega T) - 1|^2 d(\omega T) d\varepsilon_1, \quad (18)$$

and making use of the coefficients for $F_{10}(z)$ obtained through the design steps in Section IV-A, the impulse response coefficients of $Q_{10}^{(r)}(z)$ and $Q_{11}^{(r)}(z)$, $r = 1, 2, \ldots, R$, that will minimize P_1 can be designed using a least-squares technique. Due to space limitation, the procedure to derive the closed-form solution, $\alpha_1^{(r)}(k)$, for minimizing P_1 in (18) is not provided here.

V. Design Example

In this section we consider the design of a reconstructor with $\omega_0 T = 0.9\pi$, $\varepsilon_1 \in [-0.1, 0.1]$, and $P_1 = -93$ dB. The specification is chosen so as to compare the complexity of the current design with that in [5] and [6]. The value of P_1 considered in this example corresponds to an error of -100 dB, if the error power measure in [6] is used. First, the coefficients of the subfilter $F_{10}(z)$, that can be used for all time-skew errors between $\varepsilon_1 = -0.1$ and $\varepsilon_1 = 0.1$, are obtained by following the design steps in Section IV-A. Next, the subfilters $Q_{10}^{(r)}(z)$ and $Q_{11}^{(r)}(z)$ are designed as mentioned in Section IV-B. The lengths of the impulse responses of $F_{10}(z)$, $Q_{10}^{(r)}(z)$, and $Q_{11}^{(r)}(z)$ required to meet the specification in this example, turned out to be 44, 4, and 3, respectively, with $R = 3$. Implementing the reconstructor using the structure in Fig. 5(a) would require 54 fixed and 3 variable multipliers operating at half the input rate. Instead, the structure in Fig. 5(b) would need 41 fixed and 6 variable multipliers. While the structure in Fig. 5(a) needs fewer variable multipliers compared to that in Fig. 5(b), the latter structure helps to reduce the total number of multipliers. Table I shows the total number of multiplier operations at half the input rate if the reconstructor is implemented using the design approach in this paper as well as those mentioned in [5], [6], and [7]. Although the order of the reconstructor designed using the proposed method is somewhat higher than that obtained using [6], the former needs fewer multipliers. Even if the regular reconstructor in [5] has fewer multipliers among all the cases, it should be noted that all these multipliers are variable multipliers and need online redesign if the time-skew error varies. The number of fixed and variable multipliers in the proposed method is comparable to that obtained using [7]. However, the reconstructor in [7] requires online redesign when the time-skew error varies. Figure 6 shows the magnitude of $|A_1(j\omega T) - 1|$ at $\varepsilon_1 = 0.1$, for the filter obtained using the proposed method.

TABLE I
Comparison of complexity for design example.

Design approach	Order	Multipliers	
		Fixed	*Variable*
Regular [5]	40	0	41
Polynomial based [6]	44	67	3
Two-rate based [7]	44	42	7
Proposed [Fig. 5(a)]	46	54	3
Proposed [Fig. 5(b)]	46	41	6

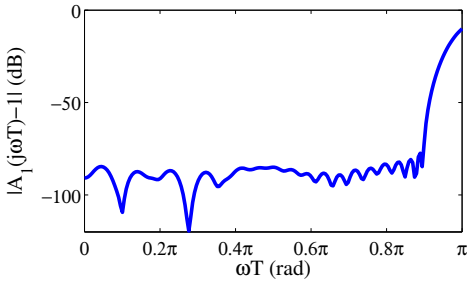

Fig. 6. Plot of $|A_1(j\omega T) - 1|$ versus bandwidth of the reconstructor in the design example, for $\varepsilon_1 = 0.1$.

VI. Conclusion

The reconstructor design approach proposed in this paper provides significant saving in the total number of multipliers needed to implement the reconstructor. Also, by eliminating the need for online redesign, we obtain more savings in terms of chip area and power consumption of the extra logic that would have otherwise been required. Two possible structures that can be used to implement the designed filter were also suggested. The structure with fewer variable multipliers can be used, for example, to reduce the power consumption due to coefficient updates or if implementing variable multipliers is costly. When all the multipliers are implemented with general multipliers, the structure with more variable multipliers and fewer total number of multipliers will be suitable.

References

[1] W. C. Black and D. A. Hodges, "Time interleaved converter arrays," *IEEE J. Solid-State Circuits*, vol. 15, no. 6, pp. 1022–1029, 1980.

[2] C. Vogel, "Modeling, identification, and compensation of channel mismatch errors in time-interleaved analog-to-digital converters," Ph.D. dissertation, Graz University, Graz, Austria, 2005.

[3] T.-H. Tsai, P. J. Hurst, and S. H. Lewis, "Bandwidth mismatch and its correction in time-interleaved analog-to-digital converters," *IEEE Trans. Circuits Syst. II*, vol. 53, no. 10, pp. 1133–1137, Oct. 2006.

[4] S. Saleem and C. Vogel, "Adaptive compensation of frequency response mismatches in high-resolution time-interleaved ADCs using a low-resolution ADC and a time-varying filter," in *Proc. IEEE Int. Symp. Circuits Syst.*, 2010, pp. 561–564.

[5] H. Johansson and P. Löwenborg, "Reconstruction of nonuniformly sampled bandlimited signals by means of time-varying discrete-time FIR filters," *EURASIP J. Advances Signal Process.*, vol. 2006, 2006.

[6] H. Johansson, P. Löwenborg, and K. Vengattaramane, "Least-squares and minimax design of polynomial impulse response FIR filters for reconstruction of two-periodic nonuniformly sampled signals," *IEEE Trans. Circuits Syst. I*, vol. 54, no. 4, pp. 877–888, Apr. 2007.

[7] A. K. M. Pillai and H. Johansson, "Efficient signal reconstruction scheme for time-interleaved ADCs," in *Proc. IEEE Int. Northeast Workshop Circuits Syst. Conf.*, Montreal, June 2012.

[8] P. P. Vaidyanathan, *Multirate Systems and Filter Banks*. Prentice-Hall, Englewood Cliffs, NJ, USA, 1993.